PERGAMON

Solid State Communications 120 (2001) 149–153

solid state communications

www.elsevier.com/locate/ssc

Study of structural changes in amorphous As_2Se_3 by EXAFS under in situ laser irradiation

Gang Chen[a], Himanshu Jain[a,*], Syed Khalid[b], Jun Li[c], David A. Drabold[c,d], Stephen R. Elliott[d]

[a]*Department of Materials Science & Engineering, Lehigh University, 5 East Packer Avenue, Bethlehem, PA 18015-1539 United States*
[b]*Brookhaven National Lab, NSLS Bldg. 725D, PO Box 5000, Upton, NY 11973-5000 United States*
[c]*Department of Physics and Astronomy, Ohio University, Athens, OH 45701-2979 United States*
[d]*Department of Chemistry, University of Cambridge, Cambridge, United Kingdom*

Received 14 June 2001; accepted 10 August 2001 by R. Phillips

Abstract

We have used the Extended X-ray Absorption Fine-Structure (EXAFS) analysis to study the in situ changes in the local atomic structure, which are induced by bandgap laser (wavelength = 690 nm) irradiation of glassy As_2Se_3. The results indicate both the temporary and permanent light-induced changes in the atomic configuration around the Se but not the As atoms. Thus the Se–Se 'defect' bonds are the primary sites of the light-induced structural changes. © 2001 Elsevier Science Ltd. All rights reserved.

PACS: 42.70.Gi; 77.84.Bw; 61.10.Ht

Keywords: A. Disordered systems; A. Chalcogenide glasses; C. EXAFS; D. Radiation effects; D. Photoinduced phenomena

1. Introduction

Semiconducting chalcogenide glasses (e.g., Se, sulfides or selenides of Ge, Sb or As, etc.) have been studied for many years because of the variety of metastable changes that they exhibit when illuminated by bandgap or sub-bandgap light [1,2]. Under irradiation, electrons and holes are created, which can become trapped or localized in the band tail states of amorphous semiconductors. Such localized states exhibit a strong electron-phonon coupling which may lead to changes in the local structure of the materials, and hence also in the physical properties causing, for example, photodarkening, photocrystallization, photo-expansion, etc. [3–6]. The recently reported opto-mechanical effect that could be applied to nanotechnology indicates the importance of such photostructural changes [7].

EXAFS is one of the very few experimental techniques that can provide atomic scale information regarding the photo-induced structure changes in these semiconducting materials. It is sensitive to local atomic structure and hence can be a powerful tool for probing the photostructural changes in chalcogenides [8,9]. Most previous EXAFS experiments for studying photostructural changes were conducted ex situ, where the structure of the glass was determined in the as-prepared stage and then after the sample was irradiated separately [10–12]. So the information about temporary structural changes "during irradiation" was not detected. Recently Kolobov et. al performed in situ EXAFS experiments on a-Se films at 30 K. They observed a light-induced increase of the average coordination number (about 5%) during Xe lamp illumination [9]. They attributed this change to the formation of dynamic interchain Se–Se bonds via interaction of excited lone-pair electrons. Simulations have essentially confirmed this picture, and have revealed that thermally induced charge fluctuations are responsible for the inter-chain bond formation in the light-excited state [13]. In this paper, we report the temporary as well as irreversible or permanent light-induced changes in glassy As_2Se_3 as observed by in situ Se and As K-edge EXAFS.

* Corresponding author. Tel.: +1-610-758-4217; Fax: +1-610-758-4244.

E-mail address: H.Jain@lehigh.edu (H. Jain).

PII: S0038-1098(01)00354-4

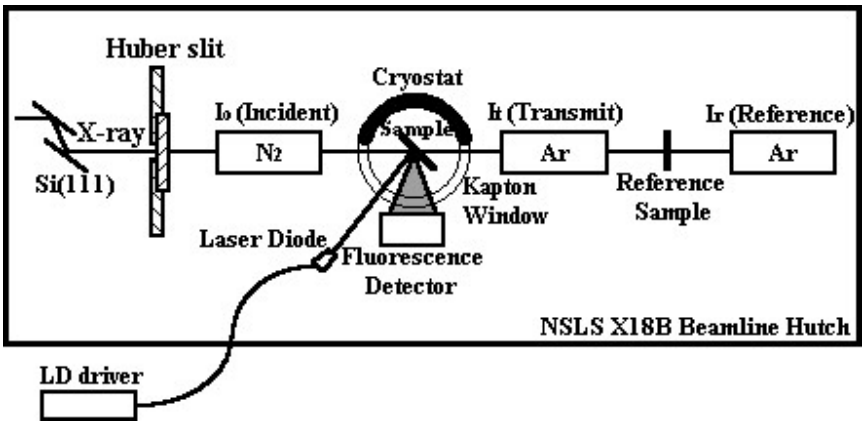

Fig. 1. Experimental setup for in situ EXAFS.

2. Experiment

Fine glassy As_2Se_3 powder[1] (99.999% purity on metal basis, 325 mesh) was used for EXAFS measurement at the National Synchrotron Light Source (NSLS) on the beamline X18B with a Si(111) channel cut double-crystal monochromator. The detuning and glitch shifting devices in the monochromator with the piezo-driven picomotors significantly improved the stability of incident X-rays. Harmonic rejection was accomplished by detuning the monochromator to 50% of its maximum flux. Data were taken in both transmission and fluorescence mode. To eliminate sample inhomogeneity, which is the largest source of noise in transmission mode, we weighed certain amount of powder, pressed and sealed it between two adhesive tapes. Then several such layers were put together to optimize the signal-to-noise ratio. The effective sample thickness was estimated to be 20–30 μm. A large area Passivated Implanted Planar Silicon (PIPS) detector was used for measuring the fluorescence signal. Two layers of eight micron thick, double sided aluminized Mylar sheets were placed on the PIPS detector to make it opaque for the hutch light, because the detector is light sensitive.

The experimental setup is shown schematically in Fig. 1. The sample was mounted on a copper holder in a closed cycle helium cryostat, equipped with kapton windows for passing X-rays and laser light. A 690 nm diode laser with 30 mW maximum output power was used for in situ illumination, and the light intensity on the sample was estimated to be 100–150 mW/cm^2. The laser diode driver was extended outside of the beamline hutch so that we could operate the laser by remote control. Standard As foil was placed before the reference ion chamber to calibrate the As K-edge of As_2Se_3 for each scan. The X-ray beam size (0.5×2 mm^2) was smaller than the laser beam size. The laser beam was adjusted to intersect the X-ray beam at a uniform region of the sample.

The EXAFS spectra were obtained for the As K-edge (11867 eV) and Se K-edge (12658 eV) in the same scan in transmission and fluorescence modes at room and 40 K temperatures. It took about one hour to complete each scan. The procedure for in situ laser irradiation was as follows. First, several consecutive spectra were taken in the dark, then the laser was turned on, irradiating the sample for 4 hours during which the EXAFS spectra were recorded at regular intervals Then, the laser was switched off and the EXAFS spectra were again recorded several times.

Fig. 2 shows raw EXAFS spectra at room temperature for both As and Se K-edge in transmission and fluorescence modes. Good sample homogeneity and a stable high-brilliance synchrotron light source, as well as a high performance ion chamber and a PIPS detector make the precision of the in situ EXAFS to be ±0.5% for a given sample under different light exposure conditions. The data show that X-ray exposure alone does not produce any detectable photostructural changes.

3. Data Analysis and Results

The K-edge of the normalized EXAFS in the single-scattering approximation can be described by [14],

$$\chi(k) = -\sum_i A_i(k)\sin[2kR_i + \varphi_i(k)] \quad (1)$$

where the summation extends over i coordination shells at average distance R_i from the absorbing atom, k is the photoelectron wave vector, and $\varphi_i(k)$ is the total phase shift due to contributions from both the absorbing and the back-scattering atoms. The amplitude function $A_i(k)$ is given by

$$A_i(k) = \frac{N_i}{kR_i^2} F_i(k)\exp(-2\sigma_i^2 k^2)\exp(-2R_i/\lambda) \quad (2)$$

where N_i is the average number of scattering atoms, $F_i(k)$ is

[1] Alfa Aesar, A Johnson Matthey Company, Ward Hill, MA, USA

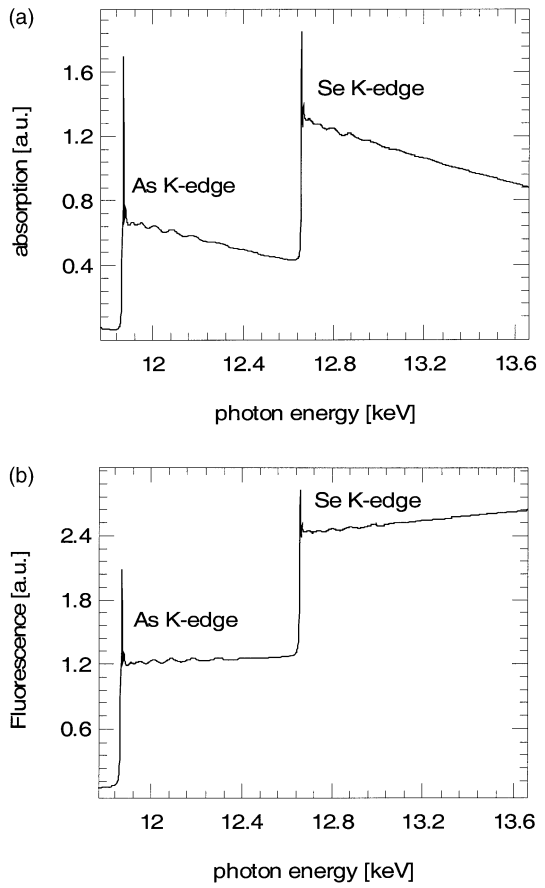

Fig. 2. As and Se K-edge transmission (a) and fluorescence (b) spectra for glassy As_2Se_3 at room temperature. These two spectra were taken during the same scan.

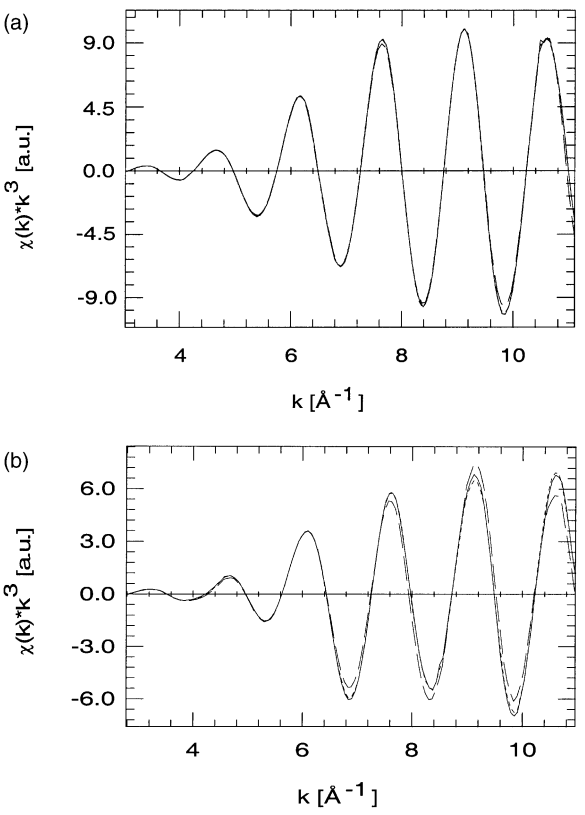

Fig. 3. Plots of As K-edge (a) and Se K-edge (b) EXAFS oscillations $\chi(k)$, multiplied by k^3, plotted as a function of photoelectron vector k before laser illumination (solid line), during illumination (dashed line) and after illumination (dotted line). Note that the before and after illumination curves almost overlap.

the backscattering amplitude characteristic of a particular type of scattering atom, σ_i^2 is the Debye–Waller factor or mean square relative displacement (MSRD) that accounts for thermal vibrations and static disorder, and λ_i is the mean-free path of the photoelectron.

Expressions (1) and (2) are used by the WINXAS program [15] for data refinement and simulation. Backscattering amplitude $F_i(k)$, phase shift $\vartheta_i(k)$ and λ_i are taken from FEFF program [16] output file, which is derived from a standard ab initio multiple scattering calculation [17]. The input file based on the As_2Se_3 crystal structure [18] for FEFF is created by the ATOMS [19] software.

EXAFS oscillations for the As and Se K-edges before, during and after laser illumination at room temperature in air were extracted from the raw spectra as shown in Fig. 3. The k^3 weighted EXAFS oscillations were Fourier transformed using the region from $k = 2.7$ to 11.7 Å^{-1} for the As K-edge, and from $k = 3$ to 12.5 Å^{-1} for the Se K-edge. The transformed spectra are shown in Fig. 4, and the structural parameters obtained by FEFF fitting are shown in Table 1. Qualitatively similar results were obtained when the samples were illuminated at 40 K in vacuum, except that in this case a small increase in laser-induced disorder was also observed around As atoms. Further analysis of the low temperature data is currently in progress and will be presented in a future publication.

The experiments were repeated on several samples, and the results of the observed changes are highly reproducible. In our in situ EXAFS experiments in transmission mode, the error is mainly form the statistical variation of counting rate and white noise, etc. Its magnitude is quite small, within $\pm 0.5\%$, as confirmed by comparing consecutive spectra for a fixed set of sample condition.

4. Discussion

From Fig. 4 we note that during bandgap laser illumination, there is no detectable change around As atoms, while the first shell peak around Se atoms decreases reversibly. By comparing our Fourier transformed spectrum for the Se K-edge with that of a-Se film obtained by another group [9], we find a difference: in the present case, the first

Table 1
Results of the fits to As and Se K-edge EXAFS before laser illumination (BI), during illumination (DI) and after illumination (AI)

	As(BI)	As(DI)	As(AI)	Se(BI)	Se(DI)	Se(AI)
R(Å) ± 0.01	2.42	2.42	2.42	2.41	2.41	2.41
Normalized CN ± 0.005	1	0.999	0.998	1	0.983	0.996
Normalized MSRD ± 0.005	1	0.996	1.002	1	1.029	1.009

shell peak of the spectrum decreases reversibly, whereas for a-Se, it increases during photoexcitation. That means a different mechanism may operate for these two cases.

According to the fitting results in Table 1, there is no change in the *average* nearest neighbor (NN) distance for either As or Se atoms. We also find that during illumination, the average coordination number (CN) of Se atoms decreases (1.7%) and the Debye–Waller factor (σ^2) or so-called mean square relative displacement (MSRD) of Se increases (2.9%) whereas no such change occurs around As atoms. Note that we placed together four layers of As_2Se_3 powder for EXAFS measurement, while the first two layers alone absorbed 97% of the laser beam. Thus the laser induced average change in CN and the MSRD should be about twice as much as the value given in Table 1.

In general, the CN and MSRD parameters are strongly correlated in EXAFS analysis. For example, Table 1 shows

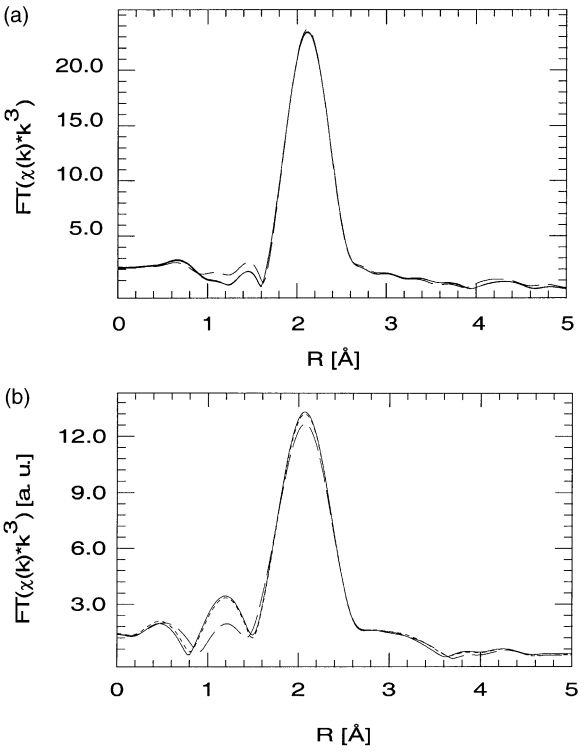

Fig. 4. Fourier transformed EXAFS spectra taken at the As K-edge (a) and Se K-edge (b) before (solid line), during (dashed line) and after laser illumination (dotted line).

a 2.9% increase in the MSRD of Se upon illumination of light when both the CN and the MSRD are allowed to vary. However, if we fix the value of CN, the increase in MSRD is calculated to be 3.6%. Next, if we correct it for the fact that the laser interaction volume is about half of that analyzed by EXAFS, this increase is 7.2%. In any case, for the purpose of present discussion, we can safely conclude that laser illumination causes a significant increase in the local disorder around Se without altering its average NN distance. However, there is no laser-induced change of CN or MSRD around the As atoms. So we conclude that to begin with there must be Se-Se defect bonds in the powder, and that the light induced structural modification occurs only in these Se–Se bonds. After switching off the laser, the enhanced disorder around Se atoms recovers for the most part, although after the first illumination there is also a small permanent increase in the disorder that does not recover when the laser is switched off.

In ideal case, the coordination number for As and Se should be 3 and 2 respectively. However, in chalcogenides glasses, the "wrong coordination" always exists. In a-Se film, it is reported that about 20% Se atoms are 3-fold coordinated [9], and first-principles molecular-dynamics calculations show [20] that in g–As_2Se_3 19.4% and 20.2% of Se atoms are in 3-fold and 1-fold coordination, respectively. However only 1.2% and 2.3% of As atoms are in 2-fold and 4-fold coordination, respectively. Our results indicate that distortion of Se–Se bond is the source of observed temporary photostructural changes in glassy As_2Se_3 caused by the bandgap light.

Our work is relevant to current theory work in the area. Li and Drabold [21] found that homopolar bonds (either As–As or Se–Se) were strongly implicated in photostructural arrangements in g–As_2Se_3. The key defects (e.g., those giving rise to localized defect states in the band tails) were coordination defects of As and Se. The former are quite rare: e.g., only one out of 86 As atoms occurs in the model). They noted that a light-induced boost of an electron from the top of the occupied tail states to the bottom of the unoccupied states resulted in complex change including bond breaking with As atoms. At room temperature we see little, if any, change in average As coordination, whereas at low temperatures there is some evidence for such change. This leads us to speculate that the defects reported in the simulation are probably 'frozen in' at low temperatures and are not present at higher temperatures. We believe that our study is consistent with

the simulations and helps to identify which defects are present at low and room temperature, something very difficult to accomplish from simulation alone.

5. Conclusion

Reversible photostructural changes have been observed by in situ EXAFS. Under bandgap laser illumination, no change occurs in the first shell mean distance around Se and As atoms. The major light-induced change occurs in the Se–Se defect bonds in the form of local distortions. The modified Se environment mostly recovers, but a small part of the structure disorder induced by light still persists after the laser is switched off. We interpret our results in terms of recent theoretical studies on the material.

Acknowledgements

We thank the National Science Foundation for supporting this work under grants DMR 0074624 (Focused Research Group) and DMR 0081006.

References

[1] K. Shimakawa, A. Kolobov, S.R. Elliott, Adv. Phys. 44 (1995) 475.
[2] K. Tanaka, Semiconductors 32 (1998) 861.
[3] A. Ganjoo, K. Shimakawa, H. Kamiya, E.A. Davis, Jai Singh, Phys. Rev. B 62 (2000) 14601.
[4] V. Lyubin, M. Klebanov, M. Mitkova, T. Petkova, Appl. Phys. Lett. 71 (1997) 2118.
[5] Vladimir V. Poborchii, Alexander V. Kolobov, Kazunobu Tanaka, Appl. Phys. Lett. 74 (1999) 215.
[6] K. Takana, Phys. Rev. B 57 (1998) 5163.
[7] P. Krecmer, A.M. Moulin, R.J. Stephenson, T. Rayment, M.E. Welland, S.R. Elliott, Science 277 (1997) 1799.
[8] C.Y. Yang, M.A. Paesler, D.E. Sayers, Phys. Rev. B 36 (1987) 9160.
[9] A.V. Kolobov, H. Oyanagi, K. Tanaka, K. Tanaka, Phys. Rev. B 55 (1997) 726.
[10] M. Frumar, A.P. Firth, A.E. Owen, Philos. Mag. B 50 (1984) 463.
[11] L.F. Gladden, S.R. Elliott, G.N. Greaves, J. Non-Cryst. Solids 106 (1988) 189.
[12] S.R. Elliott, A.V. Kolobov, Philos. Mag. B 61 (1990) 853.
[13] X. Zhang, D.A. Drabold, Intl. J. Mod. Phys. B (2001) (in press).
[14] E.A. Stern, Phys. Rev. B 10 (1974) 3027.
[15] See http://www.winxas.de for references.
[16] See http://feff.phys.washington.edu/feff/ for references.
[17] J.J. Rehr, J. Albers, R.C. Albers, S.I. Zabinsky, Phys. Rev. Lett. 69 (1992) 3397.
[18] A.L. Renninger, B.L. Averbach, Acta Cryst. Sec. B 29 (1973) 1583.
[19] See http://feff.phys.washington.edu/~ravel/software/atoms/ for references.
[20] Jun Li, D.A. Drabold, Phys. Rev. B 61 (2000) 11998.
[21] Jun Li, D.A. Drabold, Phys. Rev. Lett. 85 (2000) 2785.